



Myc/p53 interactions in transgenic mouse mammary development, tumorigenesis and chromosomal instability

Stephen J McCormack^{1,3}, Zoë Weaver², Sandy Deming¹, Geraldine Natarajan¹, Jeff Torri¹, Michael D Johnson¹, Marek Liyanage², Thomas Ried² and Robert B Dickson¹

¹The Lombardi Cancer Center, Georgetown University Medical Center, Washington DC 20007; ²National Human Genome Research Institute, NIH, Bldg 49, Room 4A28, 49 Convent Drive, MSC 4470, Bethesda, Maryland 20892, USA

We have examined defects in mammary development and tumorigenesis in a transgenic model expressing the *c-myc* gene under the MMTV–LTR promoter. The stochastic tumors which arise from hyperplastic ductal and lobular lesions in this model are characterized by high rates both of apoptosis and of chromosomal instability. Since the p53 gene product is thought to be central in the maintenance of genomic integrity, in part due to its ability to induce apoptosis in cells harboring DNA damage, we examined its expression and possible mutation. Initially, we observed that unmutated p53 is strongly expressed in premalignant mammary glands and in mammary tumors derived from the MMTV-*c-myc* strain. We then mated the MMTV-*myc* strain to a p53-deficient strain as a means of examining the effect of this lesion on mammary development and tumorigenesis in the context of *c-myc* overexpression. A lack of both p53 alleles in the presence of *c-myc* overexpression resulted in a dramatic hyperplastic alteration in mammary gland development. Specifically, in female bitransgenic MMTV-*c-myc*/p53 null mice (MMTV-*myc*/p53^{-/-}), lobular hyperplasias were observed at almost every ductal end bud as early as 32 days of age. In contrast, only mild ductal and lobular hyperplasias were seen in MMTV-*myc* mice that contained both p53 alleles (MMTV-*myc*/p53^{+/+}); an intermediate phenotype occurred in mice with a single intact (MMTV-*myc*/p53^{+/-}) p53 allele. Mammary carcinomas arose with a high frequency in MMTV-*myc*/p53^{+/-} mice; the tumors were comparable in frequency, histology and apoptotic index to the tumors in MMTV-*myc*/p53^{+/+} mice. Also, as previously observed (Elson *et al.*, 1995), lymphomas arose with extremely short latency in MMTV-*myc*/p53^{-/-} mice, precluding study of the fate of their hyperplastic mammary lesions *in situ*. The frequency of p53 mutations in MMTV-*myc*/p53^{+/+} and MMTV-*myc*/p53^{+/-} mammary tumors and in cell lines derived from these tumors was examined by direct sequencing. No point mutations or deletions in p53 were observed in mammary tumors or cell lines from either genotype. Finally, a detailed chromosomal analysis using multi-color spectral karyotyping (SKY) revealed that there were multiple chromosomal alterations in the *c-myc*-overexpressing cells that contained either one or two unmutated p53 alleles. Variable ploidy changes, a

common translocation of chromosome 11, and other chromosomal aberrations were observed. Our data thus support an interaction between c-Myc and p53 in mammary development, but suggest that loss of p53 is required neither for *c-myc*-dependent tumorigenesis nor for *c-myc*-dependent chromosomal instability.

Keywords: *c-myc*; genomic instability; chromosome 11; mammary development

Introduction

Expression of the *c-myc* protooncogene is up-regulated in as many as 80% of all breast cancers and is amplified in approximately 20–30% of these tumors (Escot *et al.*, 1986; Bonilla *et al.*, 1988; Mariani-Constantini *et al.*, 1988). *c-Myc* is a short-lived, basic helix–loop–helix leucine zipper protein that is related to the USF and E2F transcription factor families; it regulates transcription through E-box elements. As a transactivator of transcription, it is involved in the regulation of DNA synthesis, apoptosis, cellular differentiation and cell cycle progression (Ryan and Birnie, 1996).

Deregulation of *c-myc* expression is associated with the inappropriate activation of gene transcription and has been correlated with the loss of control of the cell cycle, improper initiation of DNA synthesis and instability of the genome. Overexpression of *c-myc* in CHO cells results in amplification and rearrangements of the dihydrofolate reductase (DHFR) gene (Mai, 1994; Mai *et al.*, 1996) and probably other genes. While these results provide further evidence of the involvement of c-Myc in DNA replication, gene amplification and locus-specific genomic instability, the precise molecular bases of these actions of c-Myc are not yet known.

The mechanisms regulating *c-myc* expression during normal cell function and tumorigenesis have been under investigation in multiple laboratories. It has been demonstrated that fibroblastic cells overexpressing *c-myc* are susceptible to apoptosis and that the c-Myc protein can activate apoptosis in a p53 dependent manner (Evan *et al.*, 1992). When *c-myc* expression was activated in the absence of both normal p53 alleles, fibroblasts did not undergo apoptosis (Hermekeing and Eick, 1994). Based on these results one could hypothesize that overexpression of *c-myc* in the normal or malignant mammary gland could also drive apoptosis in a p53-dependent manner. However, any role of p53 in the normal mammary gland is currently

Correspondence: RB Dickson

³Current address: Institute for Biosciences, Biomathematics, and Biotechnology, PW-1, Rm 411, George Mason University, Prince William Campus, MSN 4E3, 10900 University Boulevard, Manassas, Virginia 20101, USA

Received 17 July 1997; revised 19 December 1997; accepted 22 December 1997

unproven since the mammary glands of p53 null mice develop, lactate, and undergo post-lactational involution (apoptosis) in fashion similar to the wild-type mice (Li *et al.*, 1996).

The p53 tumor suppressor gene is one of the most frequently mutated genes, in nearly all types of cancer (Donehower and Bradley, 1993). Furthermore, an inherited mutation of a single p53 allele in the Li-Fraumeni syndrome is associated with an increased risk of breast cancer and other tumors. p53-inactivating and dominant negative mutations result in a loss of cell cycle checkpoint control, relief from p53-dependent growth arrest, DNA repair and apoptosis, and acquisition of genomic instability (Ullrich *et al.*, 1992). p53 exhibits features of a dominant-acting oncogene when present in its mutated form but it acts as a tumor suppressor gene when its non-mutated protein is expressed (Eliyahu *et al.*, 1989). The oncogenic activity of mutant p53 suggests that its mutation may result in a gain-of-function activity in addition to loss of its tumor suppressor activity. Interestingly, some mutants of p53 also require the presence of the wild type protein to exhibit this gain-of-function activity (Harvey *et al.*, 1995).

Mutation or loss of p53 is associated with a high degree of genomic instability. In non-transformed fibroblasts from Li-Fraumeni patients, it has been demonstrated that loss of the single wild-type allele is a relatively frequent event, resulting in cellular immortalization and in the accumulation of chromosomal aberrations (Bishoff *et al.*, 1990). In another study, Li-Fraumeni fibroblasts exhibited altered G₁/S checkpoint control under certain growth conditions and the reintroduction of wild-type p53 restored functionality to this checkpoint (Yin *et al.*, 1992). In addition, restoration of this checkpoint by wild-type p53 resulted in a greatly diminished frequency of drug-selected gene amplification (Yin *et al.*, 1992). These results have been further validated in hemizygous p53⁺ fibroblasts from transgenic mice. In this system, it was also observed that the loss of the remaining normal p53 allele resulted in an increased level of genomic instability, gene amplification and disruption of normal controls on cell cycle arrest (Livingstone *et al.*, 1992).

The MMTV-*c-myc* transgenic mouse strain was the earliest transgenic mammary cancer model described (Stewart *et al.*, 1984). This strain exhibits an extended latency period of 9–12 months before stochastic tumors arise (Stewart *et al.*, 1984; Leder *et al.*, 1986; Amundadottir *et al.*, 1995). In previous experiments analogous to the design of our current study, a cross between a transgenic mouse strain that expressed *c-myc* under a CD2 (thymic-selective) promoter and p53-deficient mice demonstrated synergy between the two genes in the formation of thymic lymphomas (Blyth *et al.*, 1995). In addition, a second bitransgenic mouse study confirmed the cooperative interaction of these two genes for lymphogenesis but suggested a lack of their interaction in mammary tumorigenesis (Elson *et al.*, 1995). Furthermore, in this study, acquisition of defects in a hemizygous p53 genotype through gene rearrangement appeared to be a prerequisite for tumor formation in the lymphomas but not in the mammary carcinomas. We have now extended the study of interactions of these two genes in the mammary gland. First, we have investigated potential *c-myc*/p53

interactions in early stages of mammary development and neoplasia. Second, we have addressed the role of apoptosis in tumor progression. Finally, we have utilized the newly described technique of spectral karyotyping (SKY) to address chromosomal instability in *c-myc*-induced mammary tumors (Schröck, 1996a).

Results

Genetic interaction of c-myc and p53 in mammary gland development

The aim of this study was to examine *in vivo* the role of p53 in Myc-initiated mammary development and tumorigenesis using transgenic methodologies. Transgenic mammary glands from 32 day old MMTV-*myc*, p53-deficient double transgenic mice (MMTV-*myc*/p53^{-/-}) and from MMTV-*myc* mice containing either a single (MMTV-*myc*/p53^{+/-}) or both p53 alleles (MMTV-*myc*/p53^{+/+}) were initially examined. We used a whole mount analysis of mammary glands to determine if the combined loss of p53 and over-expression of c-Myc resulted in their gross, developmental alteration. Lobular hyperplasias, characterized by inappropriate growth at the terminal end-buds and ductal hyperplasias, characterized by inappropriate growth along the mammary ducts, were each observed.

Mice that were negative for the *c-myc* transgene generally developed normally, independent of the presence or absence of the p53 gene. A representative whole mount of a non-transgenic, wild type mammary gland is shown in both high and low power magnification (Figure 1a and b respectively). The MMTV-*myc* mammary glands, containing either a single or both p53 alleles, most frequently developed mammary glands characterized by multiple areas of ductal hyperplasia (Figure 1e, f, c, d, high and low power respectively). All of the MMTV-*c-myc* mammary glands of these two genotypes also displayed shortened tertiary and quaternary ducts and club-shaped terminal end buds. In addition to ductal hyperplasias, the MMTV-*myc*/p53^{+/-} and MMTV-*myc*/p53^{+/+} mammary glands also displayed lobular hyperplasias in a limited number of ductal termini. In contrast, the MMTV-*myc*/p53^{-/-} mammary glands possessed large hyperplastic lobules at every ductal terminus. These hyperplastic regions were markedly enlarged and disordered relative to the MMTV-*myc*/p53^{+/-} mammary glands containing a single functional p53 allele (compared Figure 1g, h and e, f).

We next quantified the mean areas of the hyperplasias at the ductal termini for each genotype and calculated the relative percentage of each (Table 1). Two representative animals of each genotype were analysed by six independent investigators. We used a computer based analysis to measure and score the number of normal and hyperplastic termini as described in Materials and methods and ANOVA/Student-Newman-Keuls (SNK) tests to assess the significant differences between groups. The results shown in Table 1A indicate that hyperplastic termini in MMTV-*myc*/p53^{-/-} mammary glands occurred at a 12-fold higher frequency compared to control mice (i.e. mice lacking

the *c-myc* transgene and possessing functional p53). In addition, MMTV-*myc*/p53^{-/-} mammary glands exhibited hyperplastic termini at a 40-fold higher frequency

compared to control. (Table 1A). Both results were statistically significant. Finally the mean area of the hyperplasias in the MMTV-*myc*/p53^{-/-} mice were

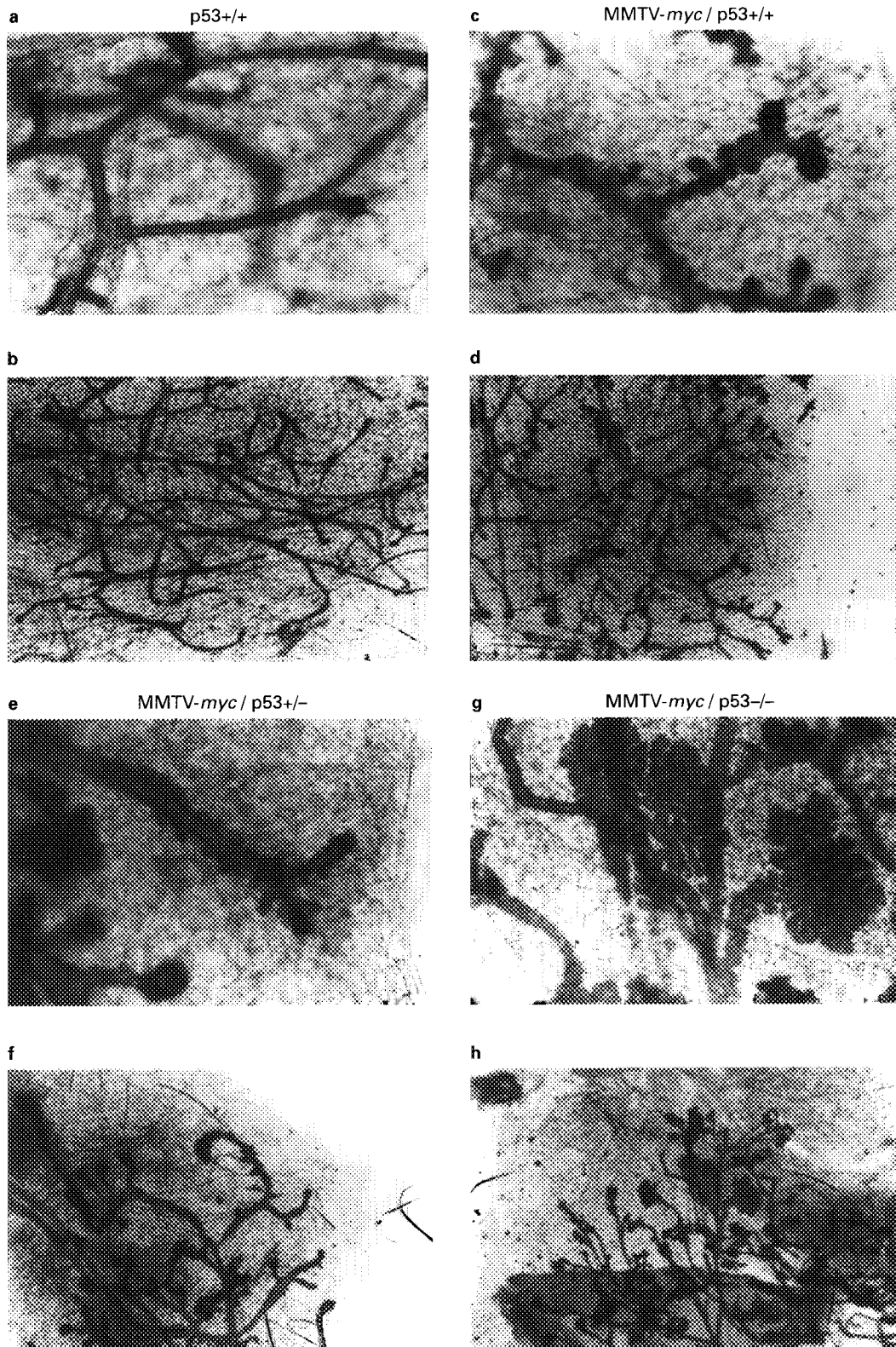


Figure 1 Development of the mammary gland in MMTV-*myc* vs MMTV-*myc*/p53^{-/-} or MMTV-*myc*/p53^{+/-} transgenic mice. A whole mount analysis was conducted on transgenic mammary glands to assess the effect of c-Myc overexpression in the presence or absence of p53. High and low power images of p53^{+/+} mice lacking the MMTV-*myc* transgene were taken as a normal reference (a and b, respectively). The MMTV-*myc* mammary epithelium displays abnormal early development and contains both ductal and lobular hyperplasias in the presence of a single or both p53 alleles (e, f and c, d, respectively). In contrast, the MMTV-*myc*/p53^{-/-} mammary glands entirely lacking functional p53 appear to be highly abnormal in early development, with large lobular hyperplasias (compare g,h to c,f, respectively)

significantly larger than those found in any of the other groups, when compared by ANOVA and Student/Newman/Keuls test (Table 1B). As noted above, a very low frequency of hyperplastic abnormalities was observed in non-transgenic mice or mice lacking the c-myc transgene but missing one or both p53 alleles. Although very infrequent, these hyperplasias were quantified for their area and presented as baseline data. These data indicate that the formation of an excess of large lobular mammary hyperplasias, in the context of c-myc overexpression, may be limited by the presence of a functional p53 allele.

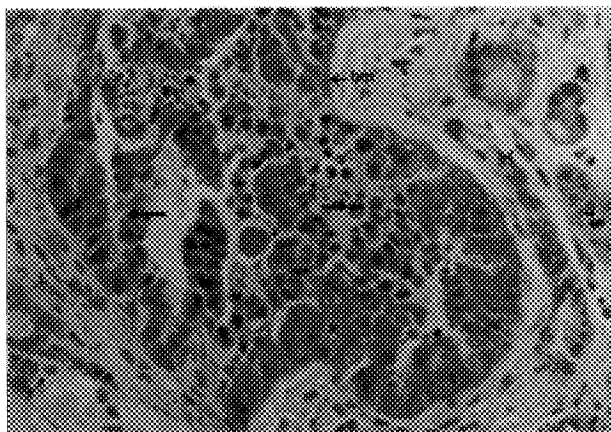


Figure 2 Histopathology of MMTV-myc/p53^{+/-} mammary tumors. Ductal hyperplasias typical of mammary epithelium of MMTV-myc/p53^{+/-} females are depicted. Apoptotic bodies (arrows) are present throughout the epithelium; in this section they are numerous. The ductal lumen (L) contains invading epithelial cells. bm = basement membrane; arrowheads point to mitotic figures. H&E stain was used for this preparation

Table 1 Morphometric analysis of hyperplasias in the ductal termini of transgenic mammary glands

A.			
p53	MMTV-myc	mean % hyperplastic end-buds	SNK groups
+/+	-	3.4 ± 5.6	I
+/-	-	4.3 ± 7.3	I
-/-	-	2.9 ± 3.6	I
+/-	+	21.1 ± 16.3	II
-/-	+	80.8 ± 13.2	III

B.			
p53	MMTV-myc	mean area (µm ²)	SNK groups
+/+	-	181.6 ± 87.0	I
+/-	-	160.9 ± 60.6	I
-/-	-	164.2 ± 79.3	I
+/-	+	200.8 ± 111.3	I
-/-	+	349.7 ± 248.3	II

Morphological differences between the ductal termini of each genotype, were quantified by measuring, in the mammary gland whole mounts, the percentage of hyperplastic termini (A) and the mean of relative area (µm²) of the ductal termini (B). The total percentage of the hyperplastic termini, the mean area, and statistical significance (at a 0.05 value) were determined as described in Materials and methods. Student/Newman/Keuls (SNK) procedure was performed to make pairwise comparisons among the means for both the percentage of hyperplastic termini and relative area. Means with the same SNK group classification (I, II, III) are not significantly different from one another. Means with different SNK group classifications differ at the 0.05 level

Tumor histology and latency in MMTV-myc p53 hemizygous mice

Evaluation of female MMTV-myc/p53^{-/-} mice for mammary tumor latency and histology was not possible since lymphomas arose with an extremely short latency, as previously described (Elson *et al.*, 1995). Therefore, the long term consequences of genetic interaction of c-myc and p53 in the mammary gland were first analysed by examining the tumor histology and latency of multiparous female MMTV-myc/p53^{+/-} mice. However, mammary tumors arising in MMTV-myc/p53^{+/-} mice were histologically similar to the tumors in the MMTV-myc/p53^{+/+} mice (Figure 2). Lymphomas and mammary neoplasias were occasionally present as combined lesions in the MMTV-myc/p53^{+/-} mice (Table 2, histology not shown).

Relationship of p53 expression and apoptosis in MMTV-myc mammary tumors

As noted earlier, one aspect in common to both Myc and p53 function is the induction of apoptosis. Histology typical of MMTV-myc/p53^{+/-} mammary tumors is shown in the hyperplastic ductal epithelium. Darkly stained, apoptotic bodies are scattered throughout the epithelium (Figure 2). To facilitate quantification of apoptosis, we also employed a histological technique which detects double-stranded breaks in DNA as the result of nucleosomal laddering (Figure 3). Many scattered cells within the MMTV-myc-induced hyperplasias and tumors were regionally positive for apoptosis. The pattern and extent of apoptosis within the MMTV-myc/p53^{+/-} tumors was similar to that which we previously described for MMTV-myc/p53^{+/+} tumors (Amundadottir *et al.*, 1996). We next conducted a statistical analysis to assess the gene dosage effect of p53 on apoptosis within MMTV-myc/p53^{+/+} and MMTV-myc/p53^{+/-} mammary tumors (see Materials and methods). The results indicated that the MMTV-myc/p53^{+/+} group was 4.3 (95% CI: 0.6, 28.8) times more likely to have a higher apoptotic score than the MMTV-myc/p53^{+/-}, although the difference is not statistically significant ($P > 0.13$).

We next utilized Western blot analysis to evaluate p53 expression and its relationship to apoptosis in the tumors and hyperplasias arising in the current study.

Table 2 Tumor type and latency in MMTV-myc/p53^{+/-} and MMTV-myc/p53^{+/+} mice

	Mammary carcinoma	Lymphoma	carc/lymph
MMTV-myc/p53 ^{+/-}			
Frequency	18/32 56%	6/32 19%	8/32 25%
Average latency = 189 ± 50 days			
MMTV-myc/p53 ^{+/+}			
Frequency	7/7 100%	0/7 0%	0/7 0%
Average latency = 196 ± 74 days			

Multiparous transgenic female MMTV-myc/p53^{+/+} and MMTV-myc/p53^{+/-} mice (2-3 pregnancies) were analysed for tumor frequency and latency. The tumor type was calculated relative to the total number of tumors as a means of assessing tumor frequency within each respective genotype. In some cases, mixed carcinoma/lymphoma lesions were observed

Hyperplastic mammary glands and tumors from MMTV-*myc* transgenic mice were rapidly frozen in LN₂, pulverized, separated by SDS-PAGE, and subjected to Western analysis using the p53 monoclonal antibody Ab421 (Figure 4a). Also, cell lines derived from MMTV-*myc* tumors were analysed by Western blot in the same fashion (Figure 4b). These results indicated that p53 is expressed at high levels in the premalignant mammary gland of MMTV-*c-myc* mice, in c-Myc-expressing primary tumors and in cell lines derived from these tumors. Mammary tumor lysates from a single transgene MT-TGF α mouse and from MDA-MB 435 human breast cancer cell lysates served as controls for low and high expression of p53, respectively (Figure 4a). Additionally, a control for normal p53 expression in an untransformed mouse mammary epithelial cell line, MMEC, was also included (Figure 4b).

To confirm p53 protein expression and to assess its localization, immunocytochemistry was conducted on MMTV-*myc/p53*^{+/+} and MMTV-*myc/p53*^{+/-} tumors. Positive staining for p53 within these tumors was regional in its localization. In all regions where p53 protein expression was detected, its localization was both nuclear and cytoplasmic (data not shown). As a control for antibody specificity, the p53 peptide

immunogen was added to a serial section of the same MMTV-*myc/p53*^{+/-} tumor in parallel with the p53 antibody; the addition of this peptide competitor resulted in a significant diminution of the immunostaining for p53 protein, as expected (data not shown).

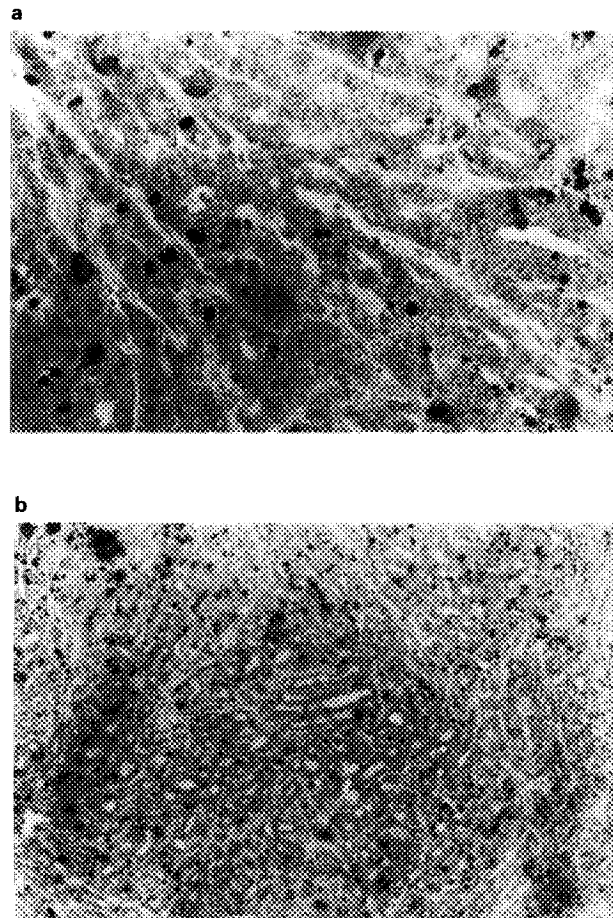


Figure 3 Detection of apoptosis in MMTV-*myc/p53*^{+/-} bitransgenic tumors. Mammary tumors from MMTV-*myc/p53*^{+/-} mammary glands, containing a single p53 allele, were analysed for apoptosis as compared to MMTV-*myc/p53*^{+/+} tumors, using an *in situ* cell death detection kit. The apoptotic staining within the MMTV-*myc/p53*^{+/-} tumors is shown in both high (400 \times) and low power (100 \times) as indicated below (a and b, respectively)

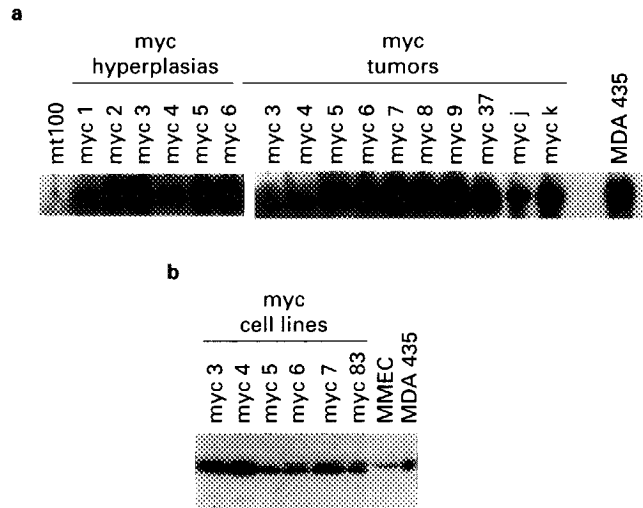


Figure 4 Western immunoblot analysis of p53 expression in mammary hyperplasias and tumor lysates from MMTV-*myc* transgenic mammary tumors and hyperplasias. The p53 protein is overexpressed in MMTV-*myc* hyperplasias and tumors. Tumors, hyperplasias and cell lysates were prepared as described, analysed by 7.5% SDS-PAGE, transferred to nitrocellulose and exposed to a p53 immunoreactive mouse monoclonal antibody. The relative expression levels of the p53 protein were visualized using the ECL system a secondary anti-mouse HRP conjugated antibody and a luminescent substrate. A TGF α single transgenic tumor, MT100; six Myc hyperplasias, and 10 Myc tumors were analysed in parallel for overexpression of p53 protein (a). Cell lines that were derived from the MMTV-*myc* tumors were also analysed by Western for p53 expression levels (b). Mouse mammary epithelial cells (MMEC) were used as a control for normal p53 expression levels (b) and MDA-MB435 breast cancer cell-line was used as a positive control for overexpression p53 protein (a,b)

Table 3 Sequence analysis of p53 in *myc* tumors and cell lines

Tumors/Cells	Genotype	Genetic Status	Sequence
#7 tumor	myc/p53 ^{+/+}	wild type	full length
#11 tumor	myc/p53 ^{+/+}	wild type	full length
#34 tumor	myc/p53 ^{+/+}	wild type	full length
#66a8 tumor	myc/p53 ^{+/-}	wild type	full length
#66a9 tumor	myc/p53 ^{+/-}	wild type	full length
#66a10 tumor	myc/p53 ^{+/-}	wild type	full length
#67a2 tumor	myc/p53 ^{+/-}	wild type	full length
#67a4 tumor	myc/p53 ^{+/-}	wild type	full length
#67a6 tumor	myc/p53 ^{+/-}	wild type	full length
#129 tumor	myc/p53 ^{+/-}	wild type	full length
#4 tumor	myc/p53 ^{+/+}	wild type	exons 5-8
#7 cell line	myc/p53 ^{+/+}	wild type	exons 5-8
#9 cell line	myc/p53 ^{+/+}	wild type	exons 5-8
#83 cell line	myc/p53 ^{+/+}	wild type	exons 5-8
#66a7 cell line	myc/p53 ^{+/-}	wild type	full length
#67a3 cell line	myc/p53 ^{+/-}	wild type	full length
#67a5 cell line	myc/p53 ^{+/-}	wild type	exons 5-8
#116b cell line	myc/p53 ^{+/-}	wild type	exons 5-8

The p53 gene was isolated from MMTV-*myc/p53*^{+/-} tumors and from explanted cell lines of these tumors. The entire coding region (full length) or the mutational hot spots (exons 5-8) from multiple independent clones was sequenced as described in Materials and methods

Table 4 Summary of chromosomal aberrations found in MMTV-*myc* transgenic mammary tumors as detected by SKY

Tumor metaphase	Chromosome #	Structural aberrations	Numerical changes		
			Gains	Losses	
67a3	#1	T(5; 11) × 2	n.d.	n.d.	
			n.d.	n.d.	
			2	5	
	#3	69	T(X; 3)	3	9
			Del(10)	6	13
			Del(2)	8 × 2	14
			Del(17)	12 × 2	16
			15		
	#4	69	T(5; 11)	n.d.	n.d.
			T(X; 3)		
	#5	57	T(5; 11)	n.d.	n.d.
			Del(10)		
	#6	64	T(X; 3)	1	6
			Del(5)	2	9
				3 × 3	10
				8 × 2	11
				12	16
				15	18
					19
67a5	#1	T(5; 5)	n.d.	n.d.	
		T(11; 11)			
		T(10; 15)			
		Rb(X; 15)			
	#2	45	Rb(11; 15)		
			T(X; 2)	2	17
			Del(17)	3	
	#3	65		6	
			Dic(2; 11)	8	
			Del(11)	2	6 × 2
			marker(2)	3 × 2	13
				7	15 × 2
	#4	62		8 × 3	18 × 3
				16	
				19	
			T(16; 19)	2 × 3	1 × 2
T(12; 8)			6 × 2	5	
Del(16)			17	8	
			18	10	
		15			
		16			
		X			
66a7	#1	T(Dp11; 1) × 2	n.d.	n.d.	
		T(1; 1)			
		T(4; 7)			
		T(7; 4)			
	#2	41	T(Dp11; 1)	19	
			#3	82	8 × 2
			#4	40	T(Dp11; 1)
#5	41	T(Dp11; 1)	5		
		#6	41	T(Dp11; 1)	
116br	#1	none		2	
				3	
				4	
				9	
				12	
				13 × 2	
				16	
				17	
				18	
	#2	111	none	n.d.	n.d.
			Del(11)	3	1 × 2
	#3	90	Del(X) × 2	13	6
			marker	X	9
					10 × 3
				11	
				12 × 2	
		14 × 3			
		16 × 2			
		18			
		19			
myc	83	42	T(X; 11)	18	0
			marker(4)		

Analysis of p53 in MMTV-myc mammary tumors by DNA sequencing

To further assess the role of p53 in c-myc-induced mammary tumorigenesis, we wished to determine if it was mutated. The MMTV-myc/p53⁻ mice provide an ideal model in which to study p53 mutation since only a single functional p53 allele is present. For these studies, we have used mammary tumors from each respective genotype as well as cell lines derived from these tumors. A modified version of the single-strand conformation polymorphism (SSCP) procedure was initially used to detect mutations spanning the entire coding region of p53 (Liu and Sommer, 1995). The SSCP analysis was conducted on seven MMTV-myc/p53⁺ tumors and cell lines in the p53 mutational hot-spot region of exons 5–8 to determine if there were any point mutations that were not detected by the initial SSCP analysis. In some cases, the entire coding region of the p53 gene was also sequenced to ensure that residues outside of exons 5–8 were not altered (Table 3). In all instances, the p53 gene was observed to be not mutated. A p53-specific RT-PCR of MMTV-myc/p53⁻ tumors always revealed two distinct, amplified products with electrophoretic mobilities of 1.3 kB and 0.8 kB. DNA sequence analysis of these two species confirmed that the 1.3 kB product was wild-type p53 and revealed that the 0.8 kB product was the result of a previously uncharacterized splice between exons 1 and exons 7 of the p53 gene (see Materials and methods). It is likely that this splice product is a consequence of the *neo* transgene insertion which interrupts exons 2–6 (Jacks *et al.*, 1994).

Genomic instability of mammary epithelial cells derived from transgenic mice

Multicolor spectral karyotyping (SKY) of tumors was used to assess overall genomic stability. Following very brief primary culture, MMTV-c-myc cells containing either a single wild type p53 allele or both unmutated p53 alleles were subjected to this chromosomal analysis. SKY is a newly developed imaging technique, involving fluorescence *in situ* hybridization (FISH) with chromosome-specific painting probes, that allows simultaneous visualization of all the human or mouse chromosomes (Schrock *et al.*, 1996a; Liyanage *et al.*, 1996). The color display image produced in SKY analysis allows the identification of complex structural aberrations that would not previously have been identifiable by standard mouse chromosome banding. This technique has already been applied to mouse model systems of tumorigenesis, including one of our MMTV-myc cell cultures (Liyanage *et al.*, 1996). This MMTV-myc cell culture (myc 83) contained both intact p53 alleles and exhibited several chromosomal aberrations: a translocation T (X; 11), loss of one X

chromosome, trisomy 18 and a dicentric marker chromosome derived from chromosome 4 (Table 4; Liyanage *et al.*, 1996). To assess the contribution of p53 for the chromosomal stability of c-myc-induced mammary tumors, we next used SKY to analyse four mammary cell cultures derived from MMTV-myc/P53⁻ tumors. We observed both numerical and structural changes in the majority of cells, consistent with the high degree of genomic instability. Additionally, the tumor cell cultures were observed to be polyclonal. The majority of cells examined for tumor 66a7 were diploid and contained a translocation of chromosome 1 to a partially duplicated chromosome 11, shown in Figure 5b. This spread also contained an extra copy of chromosome 19. In the 67a5 cell line, we observed several subclones with multiple aberrations. The representative metaphase spread of one subclone shown in Figure 5c, d was hypertriploid and contained a dicentric chromosome composed of chromosomes 2 and 11 fused at the telomeric ends and a deletion of chromosome 11 (bands D and E). This subclone also had multiple numerical aberrations.

The range of numerical and structural aberrations observed in each of the five cell cultures studied is summarized in Table 4. Several classes of mutations were observed, including translocations, Robertsonian translocations, and deletions. The translocation T (Dp 11; 1) in 66a7 (Figure 5a, b) is present in all but one of the cell cultures analysed. Furthermore, this translocation is present in two copies (in 66a7 metaphase #1), indicating that this aberration preceded the tetraploidization event. Several subclones are evident in tumor 67a5 with multiple chromosomal gains and losses and translocations, some also involving chromosome 11. Tumor 67a3 contained a consistent T (5;11) and the majority of these cells were triploid. The myc 83 cell culture, which possesses both p53 alleles, contained a consistent T (X;11) involving the telomeric end of chromosome 11. It is clear that c-myc overexpression alone, and independent of p53 mutation, can cause genomic instability. Surprisingly, four of the five cell cultures analysed in our study had aberrations involving chromosome 11, with the translocation and/or duplication located at the telomeric end of the chromosome. The mouse p53 gene is located on chromosome 11 band B2-C (Buchberg *et al.*, 1989). However, our studies with a chromosome 11-specific FISH probe made from the mouse *Brcal* gene, which is located at 11D (Schröck *et al.*, 1996b), using G-banding indicate that the chromosomal breakpoint of the translocation is telomeric to both p53 and *Brcal* in at least 2 cases (66a7 and myc83) (data not shown). These data provide further evidence that the telomeric end of mouse chromosome 11, which exhibits a high degree of conservation with human chromosome 17, contains critical genes involved in both growth suppression (Plummer *et al.*, 1997) and cell transformation (Buchberg *et al.*, 1989; Mai *et al.*, 1995).

Table 4 Footnotes

Cell lines from mammary tumors 67a3, 67a5, 66a7 and 116br were analysed by 24 color FISH/Spectral Karyotyping. At least seven metaphase spreads were analysed for each tumor cell line, and several representative karyotypes are given for each cell line. The numerical changes listed are given relative to the ploidy for each cell, for example, 67a5 metaphase #2 is hyperdiploid. The abbreviations for structural aberrations are as follows: T, translocation; Del, deletion; Rb, Robertsonian translocation (chromosomes fused at their centromeres); Dic, dicentric marker (translocation in which centromeres from both chromosomes are retained); marker chromosome (structurally abnormal and cannot be identified). n.d. means not done

Discussion

Genetic and functional relationships between c-myc and p53

In our studies a bitransgenic approach was used to gain insight into the molecular and genetic interactions

between p53 and c-myc in mammary tumorigenesis. We have focused on the mechanisms of c-myc-induced alterations in gland development, tumor formation, p53 mutation and expression, and genomic instability. First, inappropriate expression of the c-myc gene results in lobular and ductal hyperplasia in early mammary gland development; removal of both p53

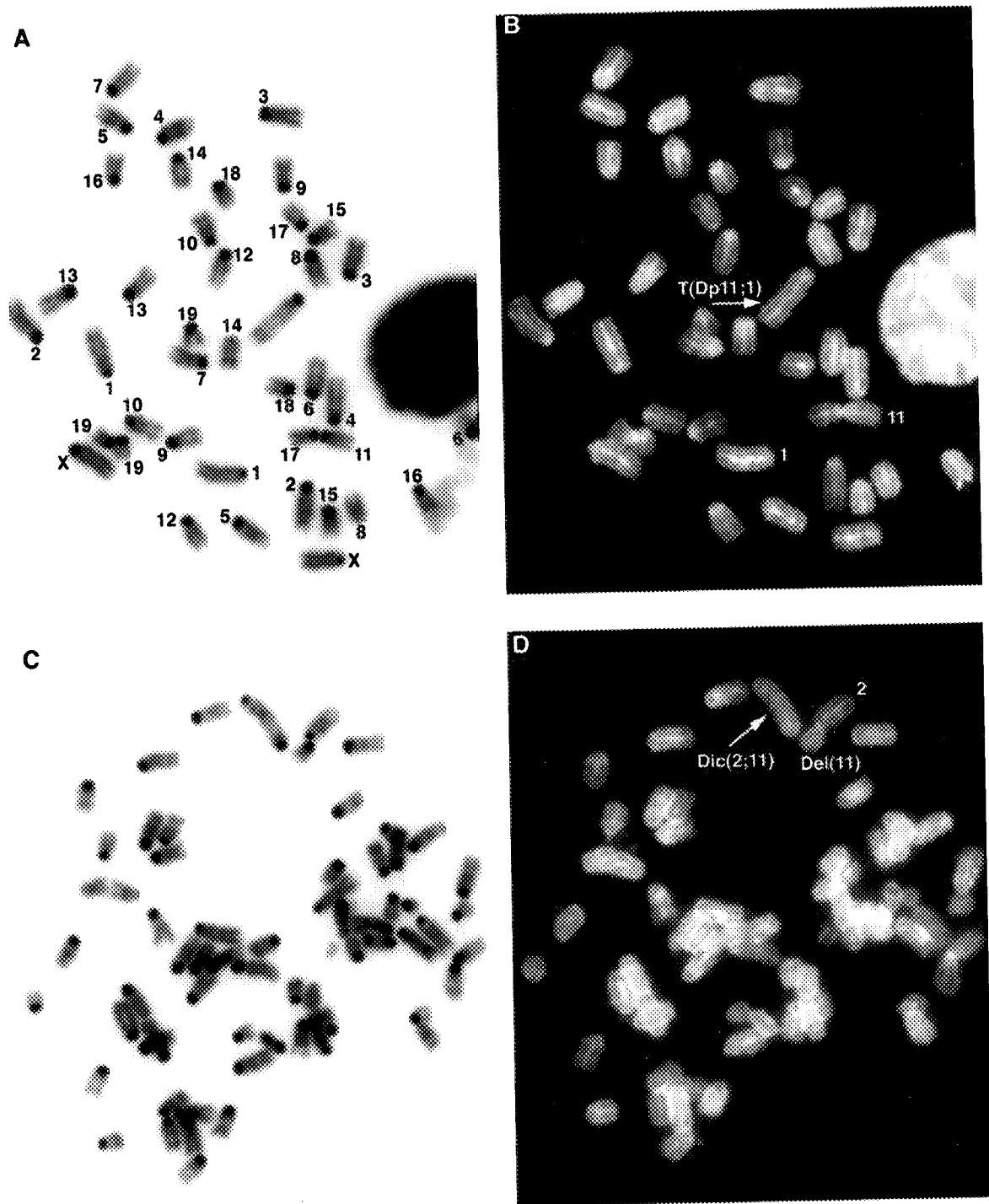


Figure 5 Spectral karyotyping of tumor cultures derived from MMTV-*myc*/p53^{+/-} transgenic mice. Spectral karyotyping was utilized to identify genomic changes that occur in low passage MMTV-*myc*/p53^{+/-} tumor cells. Representative metaphases are given for tumors 66a7 and 67a5. (a) Inverted image of a DAPI-stained metaphase spread from tumor cell line 66a7. The metaphase shown corresponds to 66a7 karyotype #2 in Table 3. All normal chromosomes are numbered. (b) The same metaphase spread shown in (a) after hybridization to the differentially labeled mouse chromosome painting probes. The T(Dp11:1) identified by the display colors is denoted by an arrow. The multicolor SKY enables easy visualization of this translocation since each specific chromosome appears in a specific color: i.e. an orange point of chromosome 11 and a light purple point of chromosome 1. (c) Inverted image of a DAPI-stained metaphase spread from tumor cell line 67a5. The metaphase shown corresponds to 67a5 karyotype #3 in Table 3. (d) The same metaphase spread shown in (c) after hybridization to mouse chromosome painting probes. The display colors for each chromosome are the same as in (b), and the aberrant chromosomes are denoted by arrows. The Dic(2;11) can be easily detected with chromosome 11 painted orange and chromosome 2 painted red

alleles in the context of c-Myc overexpression results in a dramatic amplification of the lobular hyperplastic phenotype. Second, although the formation of large, lobular hyperplasias occurs very early in mammary gland development and in a high percentage of the MMTV-*myc*/p53^{-/-} mammary glands, these aberrations appear not to be associated with acquisition of increased potential for mammary tumorigenesis. Third, in Myc-overexpressing tumors containing one or both p53 alleles, p53 appears to be strongly expressed, but its mutation has not been observed. Fourth, there was no statistical difference between the rates of apoptosis in MMTV-*myc*/p53^{+/+} and MMTV-*myc*/p53^{+/-} mammary tumors, indicating either that apoptosis may not be under critical regulation by p53 or that apoptosis is irrelevant to the progression of this model. Finally, the use of SKY has allowed the identification of several Myc-induced chromosomal aberrations. Within these c-*myc*-induced mammary tumor cells we noted a high prevalence of aberrations involving chromosome 11; the chromosomal breakpoint of at least one translocation occurred telomeric to 11D as determined by FISH mapping with a *Brcal* probe.

Mammary gland development and tumorigenesis

The mammary gland whole mount analysis of MMTV-*myc*/p53^{+/+} and MMTV-*myc*/p53^{+/-} female mice indicated that expression of the c-*myc* gene induces widespread hyperplastic abnormalities during development of the gland. In the context of a background of *myc* overexpression, we observed that the loss of a single p53 allele has little effect on the overall, large-scale pattern of mammary gland development. However, overexpression of c-*myc* in the presence of a single or both p53 alleles results in a shortening of the ducts as well as early alveolar growth along the ducts. Interestingly, these ductal abnormalities were not present in the MMTV-*myc*/p53^{-/-} mammary glands, which by contrast exhibited lobular abnormalities.

A morphometric analysis of the developmental abnormalities observed in the bitransgenic mammary glands revealed that the loss of both p53 alleles had a dramatic effect on the aberrant growth of ductal end buds (developing lobules) of MMTV-*myc*/p53^{-/-} mice by 3 weeks of age. While the MMTV-*myc*/p53^{+/-} exhibited a phenotype for these ductal terminal hyperplasias which was intermediate between that of the MMTV-*myc*/p53^{-/-} and MMTV-*myc*/p53^{+/+}, only the number of such growths (and not their size) differed significantly from the latter genotype (Table 2). Thus, there is a developmental interaction between the overexpression of c-*myc* and the absence of p53, resulting in hyperplastic growth of the mammary gland. Further investigation is required to determine whether the large hyperplasias at the ductal end buds of the MMTV-*myc*/p53^{-/-} mice are the result of a defect in cell cycle or a defect in apoptosis.

Previous work in other systems has indicated that c-Myc is involved in cell cycle regulation and that Myc can activate p53-dependent growth arrest or apoptosis (Ryan and Birnie, 1996). The latter mechanism may or may not be of significance in our model since it is only clear at present that c-Myc-induced apoptosis depends upon p53 in fibroblasts (Hermeking and Eick, 1994). In mammary epithelia, as well as other

cell types, apoptotic mechanisms may act either through p53-dependent or p53-independent pathways (Merlo *et al.*, 1995). Therefore, we might postulate that inactivation of p53, through gene knockout, selectively relieves an inhibition of Myc-mediated cell cycle deregulation. This hypothesis would parallel the findings of Hundley *et al.* (1997), who found that the combined deletion of p53 and deregulation of c-Ras^H also results in a deregulation of normal cell growth. In that study, MMTV-*ras*/p53^{-/-} bitransgenic mammary and salivary tumors had a faster rate of growth and increased genomic instability but an equivalent rate of apoptosis compared to MMTV-*ras*/p53^{+/+} and MMTV-*ras*/p53^{+/-} tumors. Also, Jones *et al.* (1997) showed in *Wnt-1*/p53^{+/-} and *Wnt-1*/p53^{-/-} bitransgenic mice that even though the two genes interacted for mammary tumor latency and frequency, this interaction correlated with increased proliferation rather than decreased apoptosis. These two sets of results suggest that in certain genetic contexts p53-mediated tumor suppression may occur independent of its apoptotic effects and may be a selective consequence of disrupted cell cycle regulation.

Our data with MMTV-*myc*/p53^{+/-} females indicate that the loss of a single p53 allele has little effect on mammary tumor latency when compared to transgenic MMTV-*myc*/p53^{+/+} females. In the earlier experiments with an analogous cross, Elson *et al.* (1995), also noted accelerated lymphogenesis but not increased mammary carcinogenesis in the absence of one or both p53 alleles. In addition to verification of these earlier results of a strong interaction of these two genes for lymphogenesis, we noted that mammary carcinomas and hyperplasias arose simultaneously as tumors of mixed histology in MMTV-*myc*/p53^{+/-} females. However, even after taking these complex tumors into account there was still no significant alteration in the latency or frequency of mammary carcinomas depending upon the p53 status.

Our analysis of p53 genetic mutation through SSCP and direct sequencing revealed that p53 is wild type both in the c-*myc* tumors and in the cell lines derived from these tumors, independent of the presence of one or two p53 alleles. Although independent lines of experimental evidence have implied that a cooperative interaction exists between the overexpression of the c-*myc* oncogene and the loss of the p53 gene in other models of experimental tumorigenesis, such as lymphomas, mutation of p53 does not appear to be a prerequisite for c-*myc*-induced tumor formation in the mouse mammary gland (Gutierrez *et al.*, 1992; Jerry *et al.*, 1994).

We observed that although it is unmutated, the p53 protein is overexpressed in both c-Myc-induced hyperplasias and tumors, indicating that its expression is a relatively early event in the tumor progression and potentially irrelevant to the tumor progression progress. In part, expression of the p53 protein could be the result of its c-Myc-mediated transcriptional transactivation. The c-Myc oncogene is known to directly activate transcription of the p53 gene through an E-box element (Reisman *et al.*, 1993), resulting in its overexpression in experimental models. In addition, c-Myc overexpression results in p53 accumulation through protein stabilization or post-translational modification (Hermeking and Eick, 1994). It has been

well established that mutation of p53 frequently results in an increase in protein stability and most clinical studies have synonymously linked p53 overexpression with genetic mutation. Alternatively, there is an emerging line of clinical evidence indicating that p53 sometimes may be overexpressed in its wild-type form (Vojtesek and Lane, 1993).

We observed that the rates of apoptosis in Myc-overexpressing tumors were high, in association with expression of the p53 protein. However, at the present time, there is no evidence that p53 plays a role in regulating this apoptosis. It is possible that the high levels of p53 in Myc-induced tumors play a much less significant role than in tumors which do not overexpress Myc. Evidence in support of this suggestion is two-fold, encompassing both apoptosis and cell cycle regulation. First, these tumors abundantly express the pro-apoptotic protein Bax (Nass *et al.*, 1996) and Bax is an independent transcriptional target of Myc (Miyashita and Reed, 1995). Second, Myc is known to induce an inhibitor of p21, the p53-induced cell cycle regulator (Hermeking *et al.*, 1995). In contrast to the studies of Donehower *et al.* (1995) whereby an allelic deficiency of p53 cooperated with the *wnt-1* transgene for mammary tumorigenesis, we and others have not noted such cooperation of p53 deficiency with the *c-myc* transgene in mammary epithelia. In addition, we should have noted frequent mutations or loss of the single p53 allele present in an MMTV-*myc* background in our studies if such a cooperation were advantageous for tumorigenesis.

Chromosomal instability and c-Myc initiated tumorigenesis

In our murine model of human carcinogenesis, it is clear that MMTV-*myc* overexpression is not sufficient for *de novo* tumor formation but that additional genetic events are required for this process to occur. Also, from these data it is clear that c-Myc overexpression, independent of p53 mutation, is associated with genetic instability and specific chromosomal rearrangements. We conducted SKY as a means of isolating specific chromosomal abnormalities that may be associated with tumor initiation and to obtain a more refined understanding of genetic instability in this model system. SKY analysis of cell lines derived from separate MMTV-*myc* tumors revealed that there was a chromosome 11 translocation in 80% of the cases. These results implicate a region that is involving or telomeric to 11D in the process of *c-myc*-initiated tumorigenesis, as determined by FISH mapping with *Brcal*. Furthermore, in previous studies with mouse plasmacytomas, a trisomy of chromosome 11 was frequently observed in addition to the T(12:15) translocation which causes deregulation of *c-myc* expression (Mai *et al.*, 1995). Interestingly, the distal region of murine chromosome 11 exhibits extensive linkage conservation with human chromosome 17 (Buchberg *et al.*, 1989) and in addition to p53 and *Brcal*, this chromosome may contain other genes involved in the tumorigenic process (Plummer *et al.*, 1997). Our future directions will include a more refined mapping of the chromosome 11 breakpoint and a continued examination of *c-myc* in the process of genomic instability.

Materials and methods

Animals

The MMTV-*c-myc* mice were of FVB background (Charles River Laboratories, MA) and the p53 knockout mice were from the 129/Sv-Trp53 strain (Jackson Labs, ME). Oligonucleotide primers for the PCR genotyping of *c-myc* and p53 mice have previously been described (Amundadottir *et al.*, 1995; Jacks *et al.*, 1994). All mice were examined twice weekly for palpable tumors and the animals were maintained according to animal guidelines. MMTV-*myc* positive females were bred to be either homozygous for the p53 wild-type allele (MMTV-*myc*/p53^{+/+}); or p53 hemizygous (MMTV-*myc*/p53^{+/-}); and MMTV-*myc* positive p53 homozygous knockout (MMTV-*myc*/p53^{-/-}). The mice used for this study were generated by crossing two MMTV-*myc*/p53^{+/-} mice. The resulting littermates had the same genetic background but differed in the status both of the p53 allele and the *c-myc* transgene. Transgenic mammary tumors and hyperplasias from the animals were formalin fixed and paraffin imbedded. Mammary epithelial cell lines were derived from mammary tumors of the MMTV-*myc*/p53^{+/+} and MMTV-*myc*/p53^{-/-} mice. Tumor bearing animals were sacrificed, tumors were removed aseptically and cell lines were prepared as previously described (Amundadottir *et al.*, 1995).

Mammary gland whole mount analysis

Virgin transgenic female mice of approximately 32 days of age were sacrificed and the inguinal mammary glands were removed and fixed on slides in 75% ethanol, 25% glacial acetic acid. After washing in 70% ETOH, and rinsing in water, the glands were stained in carmine alum solution (0.2% carmine red and 0.5% aluminum potassium sulfate, Sigma, St Louis, MO) and processed through serial alcohols. After clearing in toluene, the glands were mounted using Pennount (Sigma).

A morphometric analysis of the mammary gland whole mounts was conducted to obtain a more quantitative understanding of the relationship between phenotype and genotype. To measure that relative percentage of hyperplastic end-buds, we analysed two representative mammary gland whole mounts from each transgenic genotype and six blinded scorers determined the total number of end-buds along with the number of hyperplastic end-buds for each whole mount. Quantitative data were generated by selecting representative mammary gland whole mounts from each genotype, and three representative fields from each whole mount were examined using an image analysis system. The area of the three largest end-buds in each field was measured (Optima 5.2, Bothell, WA), providing a total of 18 area measurements for each genotype. Statistical analysis was performed using SAS 3.12 (Statistical Analysis Systems Institute Inc., Cary, NC) to examine significant differences between each of the genotypes with respect to percentage of hyperplastic end-buds and the relative area of the end-buds. One way analysis of variance, and Student/Newman/Keuls tests were performed with the Proc ANOVA and PROC MEANS/SNK functions in SAS in both cases.

Apoptosis detection in tumor sections

Mammary tumors from the transgenic mice of approximately 150 days of age, were formalin fixed, paraffin embedded and 5 micron sections were prepared as previously described (Amundadottir *et al.*, 1996). Apoptotic cells were detected using the Apotag (Oncor, Gaithersburg, MD) or In Situ cell death (Trevigen, Gaithersburg, MD) kits to identify double stranded DNA breaks. Tissue sections were deparaffinized by baking at 80°C, soaked in xylene before washing with

PBS, treated with proteinase K at 20 µg/ml, and peroxidase activity was quenched in H₂O₂ for 30 min. The assays were continued using the manufacturers instructions and the sections were counter stained with methyl green or hematoxylin. To quantify the level of apoptosis, six tissue sections of each genotype were scored by six blinded observers. Apoptosis levels were scored from 0 to + + +, with (0, +) representing low and (+ +, + + +) high scores. A proportional odds model (McCullagh and Nelder, 1989) was used to analyse data comparing apoptotic frequencies between groups.

Western analysis of p53

For Western analysis, a section of the tumors were pulverized under LN₂ before the addition of lysis buffer, 10 mM Tris pH 7.4, 1% SDS, and for the cell lines the lysis buffer was added directly to the isolated cell pellet. The protein concentration was determined using the Pierce protein assay prior to the addition of 2×Lanemeli buffer and boiling. 20 µg of total protein was analysed by 7.5% SDS-PAGE, transferred to nitrocellulose and immunoblotted with monoclonal antibody to p53 (Oncogene Sciences AB-1, PAb421). The immunoreactive proteins were visualized using the ECL detection system (NEN, Boston, MA).

Immunohistochemical analysis of p53

Paraffin-embedded, formalin-fixed tumors and hyperplasias from MMTV-*myc* and MMTV-*myc*/p53 transgenic mice were sectioned and stained for p53 using an affinity purified anti-peptide antibody directed against the N-terminus of p53 (generously provided by Dr E Appella, NIH) and an ABC kit to visualize immunoreactivity (Vector Labs, Burlingame, CA). This antibody has previously been used to successfully analyse p53 expression in murine tumors (Ueda *et al.*, 1995). The p53 immunogen (MEEPQSDPS-VEPPLSQETFSDL WKLLPE) was used to compete for the immunostaining in the tumors as has previously been described (Ueda *et al.*, 1995).

SSCP (single-strand conformational polymorphism) analysis

The p53 gene was isolated from MMTV-*myc* mammary tumors using RT-PCR, and the full-length cDNA was used in a modified SSCP analysis. This assay has been previously used for the p53 gene and is the most efficient method of assessing if p53 is mutated and also in determining the region of mutation (Liu and Sommer, 1995). Briefly, total RNA was isolated from pulverized tumors by adding 4 M guanidine thiocyanate, acid phenol extraction and precipitation with isopropanol. We isolated RNA from a non-transgenic mouse brain as a wild-type p53 control. Standard RT-PCR reactions were carried using p53 specific primers with the addition of [α -³²P]ATP to visualize the products. The amplified p53 product was digested separately with *Taq*I, *Pst*I, *Eco*47III, *Acc*I, *Blp*I and *Apal* to generate fragments of 233 base pairs and less. These products were then denatured and electrophoresed under non-denaturing conditions (Liu and Sommer, 1995). This method is advantageous because using endonucleases on the amplified gene product, followed by conventional SSCP analysis, it is possible to detect mutations across the entire gene.

References

Amundadottir LT, Johnson MD, Merlino G, Smith G and Dickson RB. (1995). *Cell Growth. Diff.*, **6**, 737-748.
Amundadottir LT, Nass S, Berchem G, Johnson MD and Dickson RB. (1996). *Oncogene*, **13**, 757-765.

Sequence analysis of p53

RT-PCR was performed on MMTV-*myc*/p53^{-/-} and MMTV-*myc*/p53^{-/-} tumors and cell lines using p53 specific primers. A single 1.3 kB PCR product was consistently amplified from cells possessing a p53^{-/-} genotype and two fragments of 0.8 kB and 1.3 kB were consistently amplified from p53^{-/-} cells. The DNA fragments were gel purified, subcloned, and sequenced using an ABI 373 Automated DNA sequencing system and the PRISM Ready Reaction Dye Deoxy Terminator cycle sequencing kit (Perkin-Elmer, Groton CT). The 0.8 kB fragments contained the sequence TTCTCCGAA-GACTGG|GCCGGCTCTGAGTAT, which appears to result from the splicing of exon 1 to exon 7. The presence of this transcript is not surprising since the *neo* gene interrupts the p53 genomic sequence between exons 2-6.

Multicolor spectral karyotyping

Mouse metaphase chromosomes were prepared from low passage MMTV-*myc* tumor cell cultures (passage 4-6) by lysis in 0.06 M KCl and fixation in methanol/acetic acid, after incubation of cells for 5 h in 0.1 µg/ml colcemid. For the hybridization probes, mouse chromosomes isolated by high resolution flow sorting were individually labelled using degenerate oligonucleotide primed PCR (DOP-PCR; Telenius *et al.*, 1992). The labeling scheme uses five different fluorochrome conjugated or haptenized nucleotides in various combinations so as to generate a unique spectral profile for each chromosome, as described previously (Liyanage *et al.*, 1996). The fluorochromes used for direct incorporation were Spectrum Orange, Spectrum Green, and Texas Red. Biotin- and digoxigenin-labelled nucleotides were detected with avidin-conjugated Cy5 and antibody-conjugated Cy5.5, respectively, after hybridization. Hybridization of the labelled probes to the metaphase spreads was carried out for 2-3 days in the presence of an excess of unlabelled Cot-1 fraction of mouse genomic DNA. Labelled chromosomes were then counterstained with DAPI. The chromosomes were imaged on an inverted microscope (Leica DMIRBE) that was equipped with a spectral cube system (SD200, Applied Spectral Imaging) and a custom designed filter set (Chroma Technology) that allows for the simultaneous excitement of all dyes and the measurement of their emission spectra. The conversion of emission spectra to visualize the spectral image in display colors is achieved by assigning a different color (blue, green or red) to specific spectral ranges.

Acknowledgements

MMEC cells were kindly provided by Dr Nitin Telang, Cornell University. This work was supported in part by a SPORE fellowship from NIH-IP5OCA58185 to SJM and NIH-RO1AG1496-01 to RBD. SJM was also supported by an NIH NRSA postdoctoral fellowship at the end of the study. We thank Dr Ettore Appella for valuable discussion, Dr Gloria Chepko for assistance with photography, tumor histopathology and critical reading of the manuscript. We also thank Dr Nicholas Kenny for histopathological evaluation of the tumors and Rebecca Slack for statistical evaluation.

Bischoff F, Yim SO, Pathak S, Grant G, Siciliano MJ, Giovanella BC, Strong LC and Tainsky MA. (1990). *Cancer Res.*, **50**, 7979-7984.

- Blyth K, Terry A, O'Hara M, Baxter EW, Campbell M, Stewart M, Donehower LA, Onions DE, Neil JC and Cameron ER. (1995). *Oncogene*, **11**, 1717–1723.
- Bonilla M, Ramirez M, Lopez-Cueto J and Gariglio P. (1988). *J. Natl. Cancer Inst.*, **80**, 665–671.
- Buchberg AM, Brownell E, Nagata S, Jenkins NA and Copeland NG. (1989). *Genetics*, **122**, 153–161.
- Donehower LA and Bradley A. (1993). *Biochim. Biophys. Acta*, **1155**, 181–205.
- Donehower LA, Godley LA, Aldaz CM, Pyle R, Shi YP, Pinkel D, Gray J, Bradley A, Medina D and Varmus HE. (1995). *Genes Dev.*, **9**, 882–895.
- Eliyahu D, Michlaovitz D, Eliyahu S, Pinhasi-Kimhi O and Oren M. (1989). *PNAS*, **86**, 8763–8767.
- Elson A, Deng CX, Campstorres J, Donehower LA and Leder P. (1995). *Oncogene*, **11**, 181–190.
- Escot C, Theillet C, Lidereau R, Spyrtos F, Champeme MH, Gest J and Callahan R. (1986). *PNAS*, **83**, 4834–4838.
- Evan GI, Wyllie AH, Gilbert CS, Littlewood TD, Land H, Brooks M, Waters CM, Penn LZ and Hancock DC. (1992). *Cell*, **69**, 119–128.
- Gutierrez MI, Bhatia K, Siwarski D, Wolff L, Magrath IT and Mushinski JF. (1992). *Cancer Res.*, **52**, 1032–1035.
- Harvey M, Vogel H, Morris D, Bradley A, Bernstein A and Donehower LA. (1995). *Nature Genetics*, **9**, 305–311.
- Hermeking H and Eick D. (1994). *Science*, **265**, 2091–2093.
- Hermeking H, Funk JO, Reichert M, Ellwart JW and Eick D. (1995). *Oncogene*, **11**, 1409–1415.
- Hundley JE, Koester SK, Troyer DA, Hilsenbeck SG, Subler MA and Windle JJ. (1997). *Mol. Cell. Biol.*, **17**, 723–731.
- Jacks T, Remington L, Williams BO, Schmitt EM, Halachmi S, Bronson RT and Weinberg RA. (1994). *Curr. Biol.*, **4**, 1–7.
- Jerry DJ, Butel JS, Donehower LA, Paulson EJ, Cochran C, Wiseman RW and Medina D. (1994). *Mol. Carcin.*, **9**, 175–183.
- Jones J, Attardi L, Godley LA, Laucirieu R, Medina D, Jacks T, Varmus H, and Donehower LA. (1997). *Cell Growth and Diff.*, **8**, 829–838.
- Leder A, Pattengale PK, Kuo A, Stewart T and Leder P. (1986). *Cell*, **45**, 485–495.
- Li M, Hu J, Heermeier K, Hennighausen L and Furth PA. (1996). *Cell Growth and Diff.*, **7**, 13–20.
- Liu Q and Sommer SS. (1995). *Biotechniques*, **18**, 470–477.
- Livingstone LR, White A, Sprouse J, Livanos E, Jacks T and Tlsty TD. (1992). *Cell*, **70**, 923–935.
- Liyanage M, Coleman A, du Manoir S, Veldman T, McCormack S, Dickson RB, Barlow C, Wynshaw-Boris A, Janz S, Wienberg J, Ferguson-Smith M, Schrock E and Ried T. (1996). *Nature Genetics*, **14**, 312–315.
- Mai S. (1994). *Gene*, **148**, 253–260.
- Mai S, Hanley-Hyde J, Coleman A, Siwarski D and Huppi K. (1995). *Genome*, **38**, 780–785.
- Mai S, Hanley-Hyde J and Fluri M. (1996). *Oncogene*, **12**, 277–288.
- Mariani-Constantini R, Escot C, Theillet C, Gentile A, Merlo G, Liderau R and Callahan R. (1988). *Cancer Res.*, **48**, 199–205.
- McCullah P and Nelder J. (1989). *Generalized linear models*. Cambridge University Press, 151–155.
- Merlo GR, Basolo F, Fiore L, Duboc L and Hynes NE. (1995). *J. Cell. Biol.*, **128**, 1185–1196.
- Miyashita T and Reed JC. (1995). *Cell*, **80**, 293–299.
- Nass SJ, Minglin L, Amundadottir LT, Furth PA and Dickson RB. (1996). *Biochem. Biophys. Res. Com.*, **227**, 248–256.
- Plummer SJ, Adams L, Simmons JA and Casey G. (1997). *Oncogene*, **14**, 2339–2345.
- Reisman D, Elkind NB, Roy B, Beamon J and Rotter V. (1993). *Cell Growth Differ.*, **4**, 57–65.
- Ryan KM and Birnie GD. (1996). *Biochem. J.*, **314**, 713–721.
- Schröck E, du Manoir S, Veldman T, Schoell B, Wienberg J, Ferguson-Smith MA, Ning Y, Ledbetter DH, Bar-Am I, Soenksen D, Garini Y and Ried T. (1996a). *Science*, **273**, 494–497.
- Schröck E, Badger P, Larson D, Erdos M, Wynshaw-Boris A, Ried T and Brody L. (1996b). *Human Genetics*, **97**, 256–259.
- Stewart TA, Pattengale PK and Leder P. (1984). *Cell*, **38**, 627–637.
- Telenius H, Pelmeur AH, Tunnacliffe A, Carter NP, Behmel A, Ferguson-Smith MA, Nordenskjöld M, Pfragner R and Ponder BA. (1992). *Genes Chromosom. Cancer*, **4**, 257–63.
- Ueda H, Ullrich SJ, Gangemi JD, Kappel CA, Ngo L, Feitelson MA and Jay G. (1995). *Nature Genetics*, **9**, 41–47.
- Ullrich SJ, Mercer WE and Appella E. (1992). *J. Biol. Chem.*, **267**, 15259–15262.
- Vojtesek B and Lane DP. (1993). *J. Cell Sci.*, **105**, 607–612.
- Yin Y, Tainsky MA, Bishoff FZ, Strong LC and Wahl J. (1992). *Cell*, **70**, 937–948.